Electronic Supplementary Material (ESI) for Materials Horizons.

Supplementary information: Giant spontaneous exchange bias in an antiperovskite structure driven by a canted triangular magnetic structure

Lei Ding,[1,*] Lihua Chu,[2] Pascal Manuel,[1,†] Fabio Orlandi,[1] Meicheng Li,[2] Yanjiao Guo,[2] and Zhuohai Liu[2]

[1] *ISIS Facility, Rutherford Appleton Laboratory, Harwell Oxford, Didcot OX11 0QX, United Kingdom*
[2] *State Key Laboratory of Alternate Electrical Power System with Renewable Energy Sources, School of Renewable Energy, North China Electric Power University, Beijing 102206, China*

* lei.ding.ld@outlok.com, lei.ding@stfc.ac.uk
† pascal.manuel@stfc.ac.uk

CONTENTS

I. MATERIALS SYNTHESIS

TABLE I. Phase purity of $Mn_{3.5}Co_{0.5}N$ samples prepared with different amount of excess of Co content.

Amount of excessive Co	$Mn_{3.5}Co_{0.5}N$	MnO	Mn_2N	CoO	Technique
0	76(1)%	7.6(4)%	10.3(4)%	6(1)%	XRD
40%	94.6(1)%	2.41(3)%	2.63(5)%	0.35(8)%	NPD
63%	87(1)%	11.4(6)%	1.9(4)%	undetectable	XRD
87%	95.6(4)%	3.37(4)%	0.83(4)%	0.25(4)%	NPD
110%	95.3(2)%	3.50(3)%	0.86(5)%	0.32(4)%	NPD

TABLE II. The occupancy of Mn^{II} and Co^{II}) atoms at the 1a (0,0,0) site in $Pm-3m$ space group, extracted from NPD

Amount of excessive Co	Mn^{II}	Co^{II}
40%	0.52(5)	0.48(5)
87%	0.51(5)	0.49(5)
110%	0.51(5)	0.49(5)

TABLE III. Structural parameters for the $Mn_{3.5}Co_{0.5}N$ sample prepared with 110% excess of Co content, refined from the neutron diffraction data collected at 500 K in the $Pm-3m$ space group.

Atom	x	y	z	B(Å^2)	Occupancy
Mn/Co	0	0	0	1.3(3)	0.51(5)/0.49(5)
Mn	0	0.5	0.5	1.10(6)	3.0
N	0.5	0.5	0.5	0.68(6)	1.0

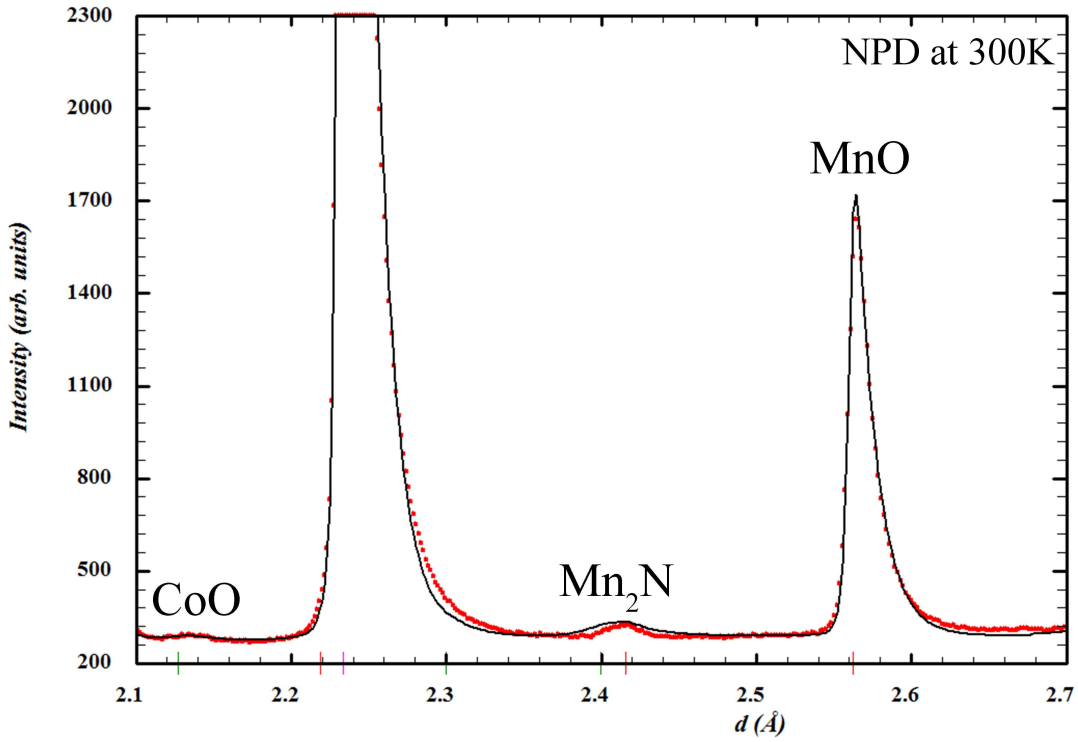

FIG. S1. Observed (black) and calculated (red) powder neutron diffraction pattern for the $Mn_{3.5}Co_{0.5}N$ sample prepared with 110% excess of Co content collected at room temperature. The reflections of the impurity phases MnO, Mn_2N and CoO are marked. It shows that the strong reflection from CoO are actually not resolution limited.

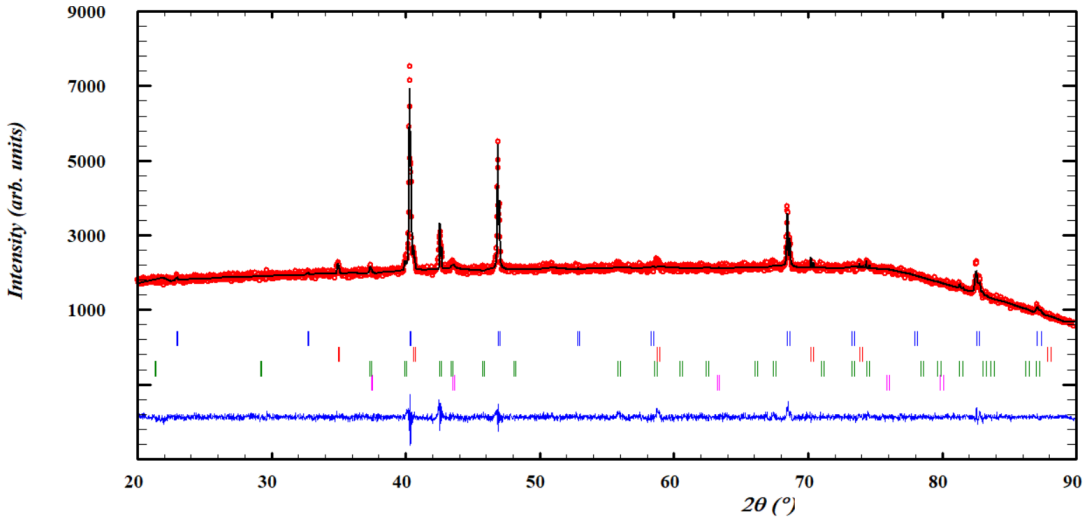

FIG. S2. Observed (red circles) and calculated (black line) powder x-ray diffraction patterns for the $Mn_{3.5}Co_{0.5}N$ sample prepared without the excess of Co content collected at room temperature. The reflections of the main phase are denoted by upper tick marks. The reflections marked in middle belong to a MnO impurity phase. The second lowest tick marks show the contribution from a Mn_2N impurity phase. The lowest ones mark CoO phase. The bottom line shows the difference between the observed and calculated patterns.

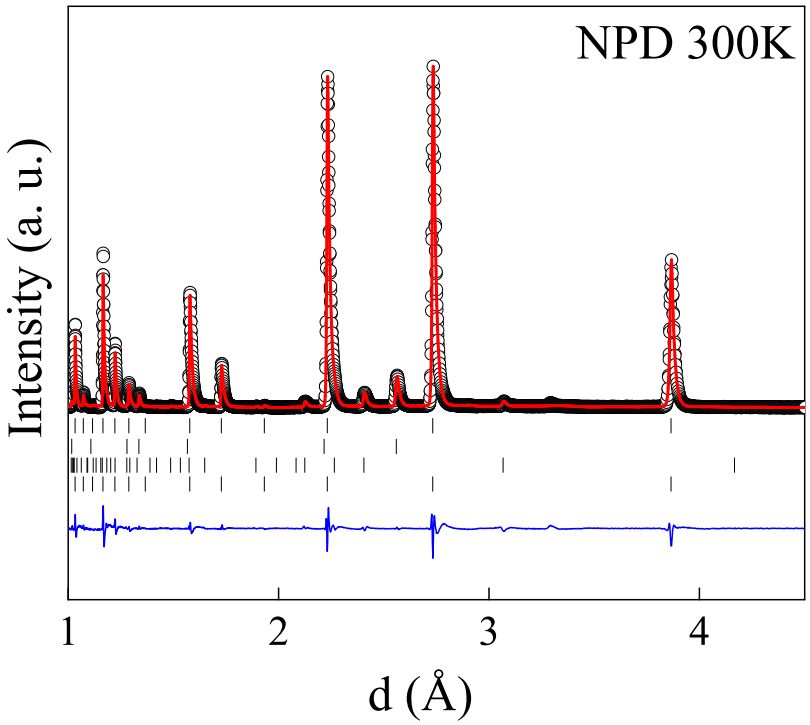

FIG. S3. Observed (open circles) and calculated (line) powder neutron diffraction patterns for the $Mn_{3.5}Co_{0.5}N$ sample prepared with 40% excess of Co (40%) collected at 300 K. The nuclear reflections are denoted by upper tick marks. The reflections marked in middle belong to MnO and Mn_2N impurity phases. The lowest tick marks show magnetic phase represented by mGM4+. The bottom line shows the difference between the observed and calculated patterns.

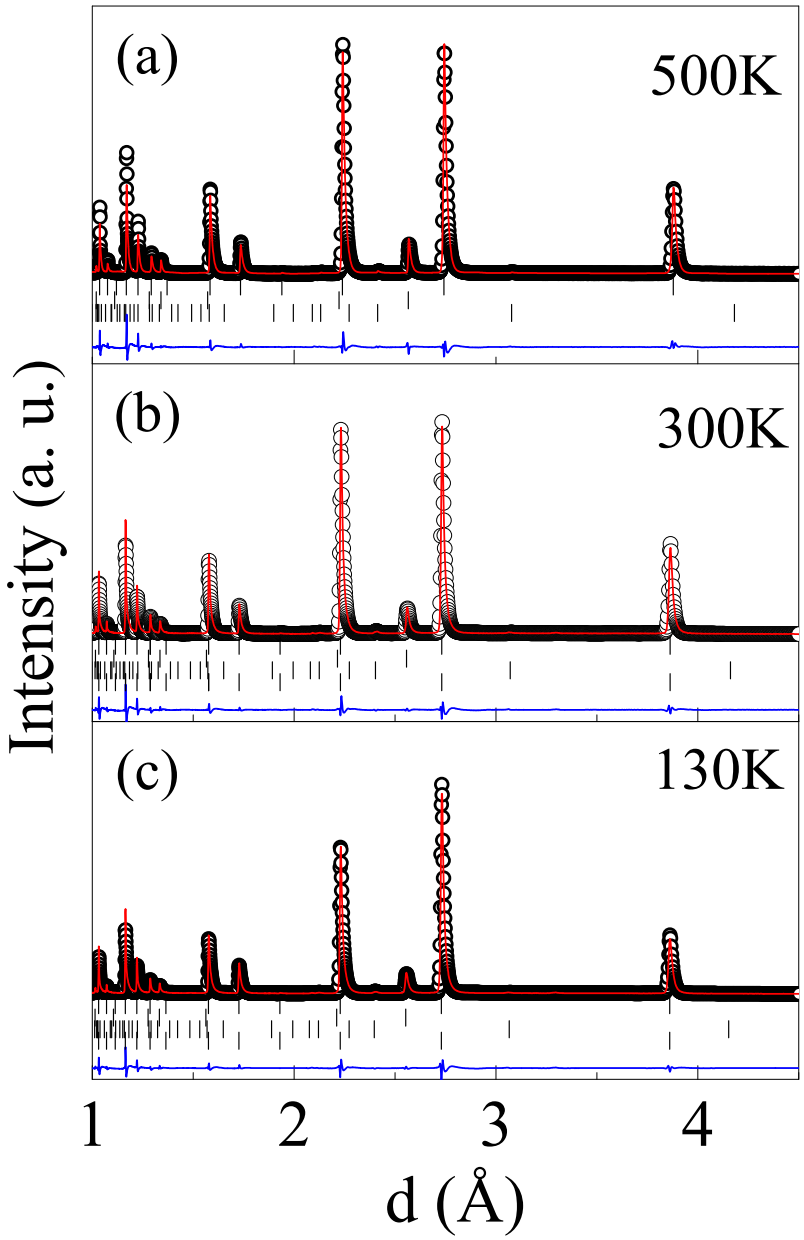

FIG. S4. Observed (open circles) and calculated (line) powder neutron diffraction patterns for the $Mn_{3.5}Co_{0.5}N$ sample prepared with 87% excess of Co content collected at 500, 300 and 130 K. The nuclear reflections are denoted by upper tick marks. The reflections marked in middle and lower panels belong to MnO and Mn_2N impurity phases. The lowest tick marks in (c) show magnetic phase represented by mGM4+. The bottom line shows the difference between the observed and calculated patterns.

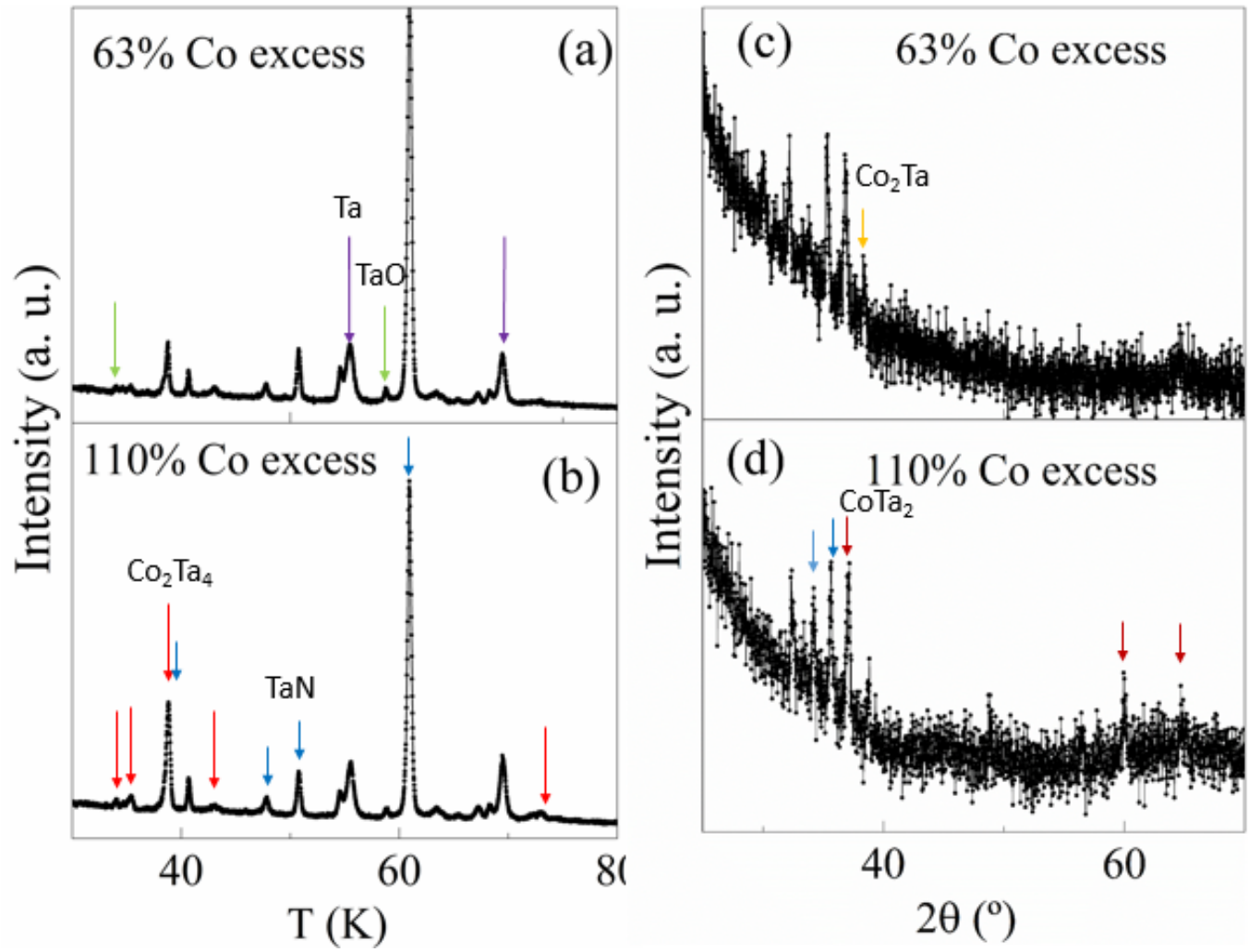

FIG. S5. XRD patterns measured on the Ta foils used in the synthesis for the samples prepared with 63% (a) and 110% (b) excess of Co content; (c)-(d) present the XRD patterns on used quartz tubes for the corresponding samples.

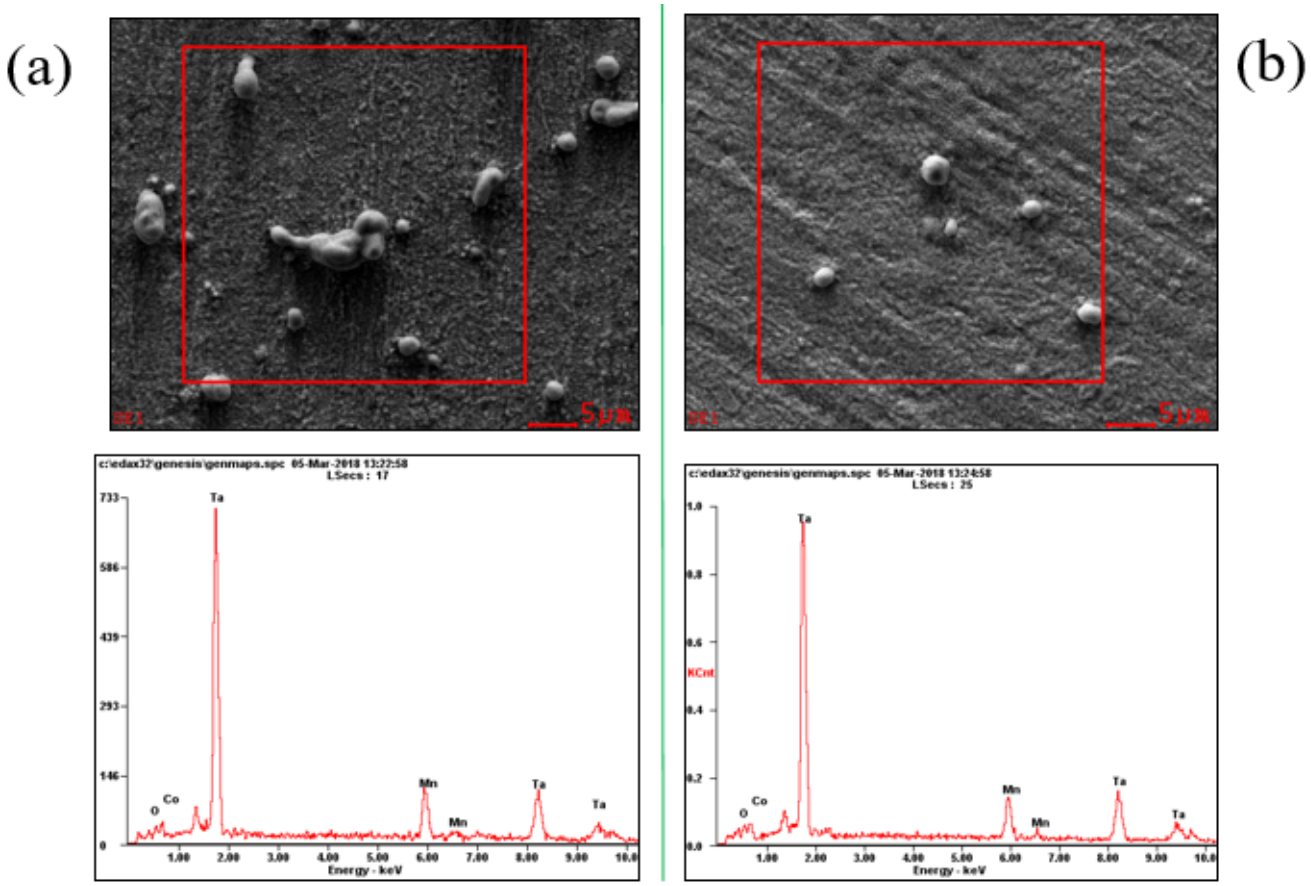

FIG. S6. SEM and EDX results measured on the Ta foils used in the synthesis for the samples prepared with 110% (a) and 63% (b) excess of Co content.

II. MAGNETIC PROPERTIES FOR SAMPLES PREPARED WITH DIFFERENT AMOUNT OF EXCESSIVE CO

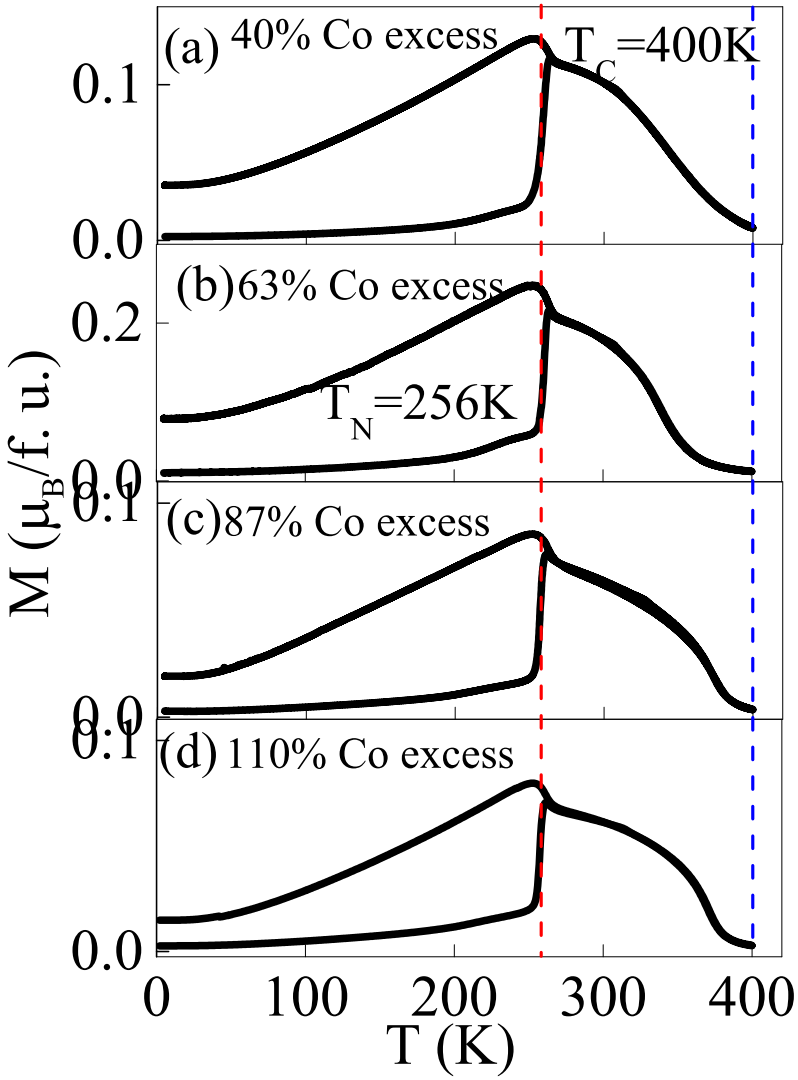

FIG. S7. Temperature dependence of the magnetization of samples prepared with different amount of excessive Co content in a magnetic field of 0.1 T under ZFC and FC conditions.

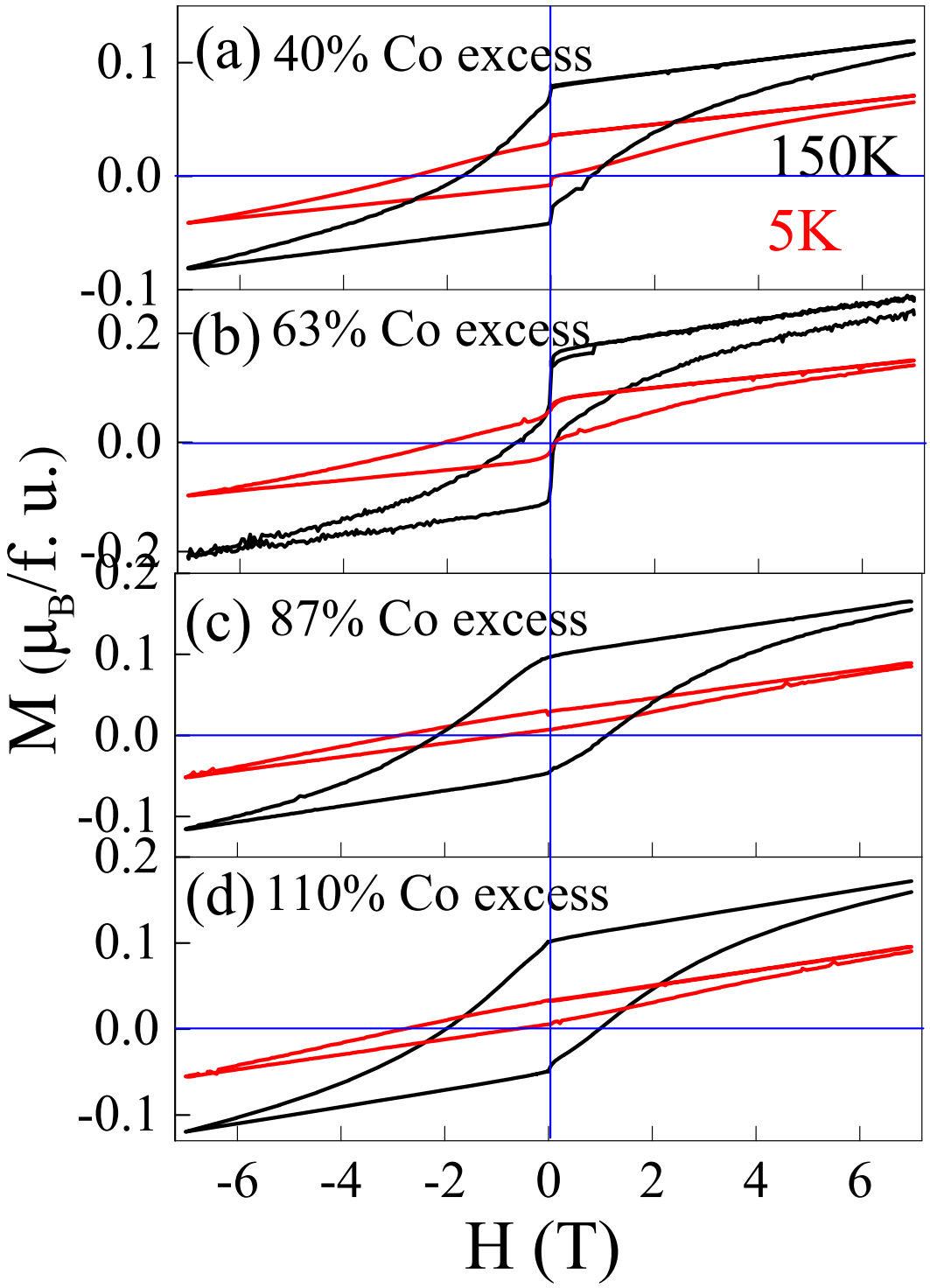

FIG. S8. Magnetic hysteresis loops for samples prepared with different amount of excessive Co content measured at 5 and 150 K after a cooling field of 1 T.

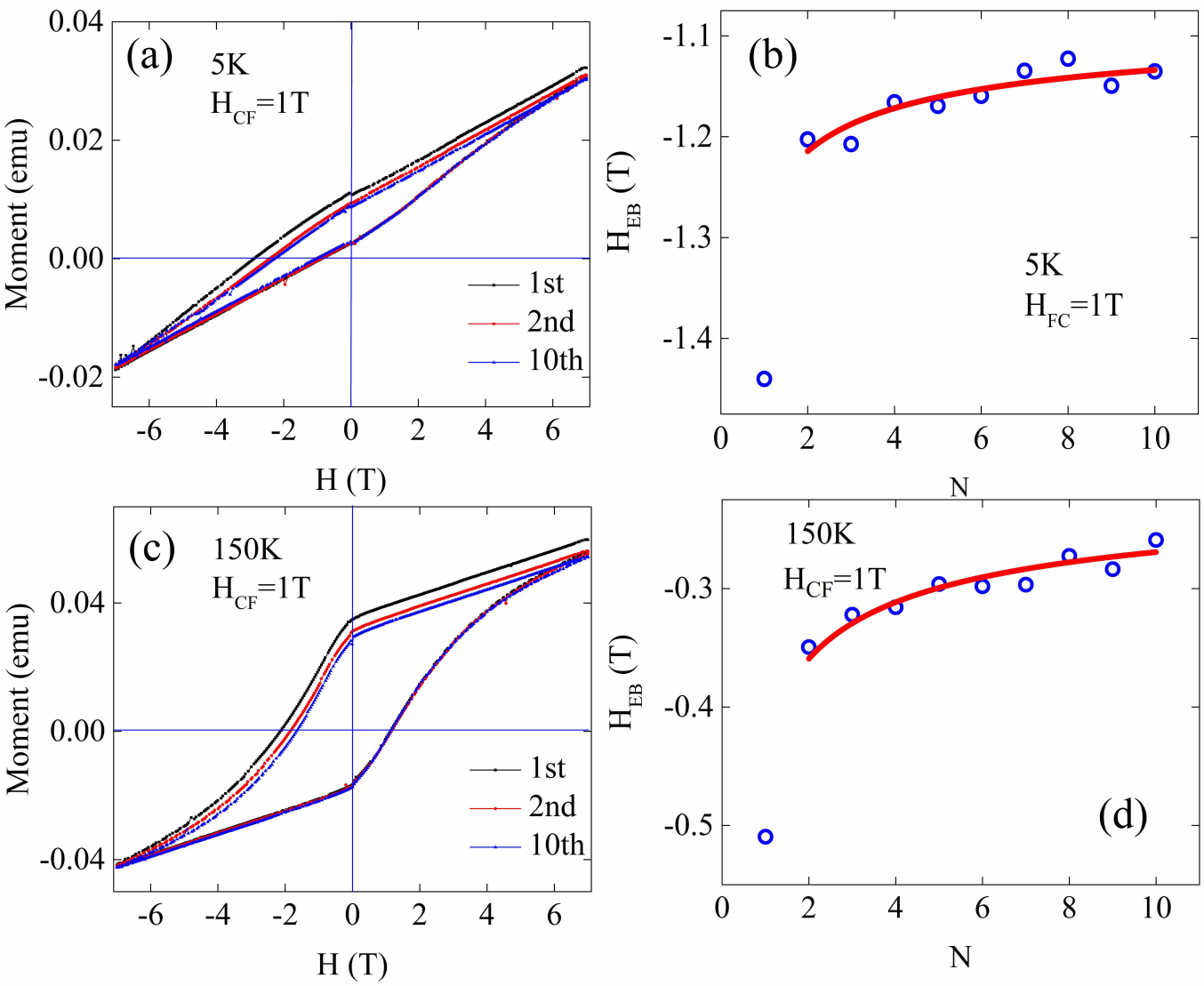

FIG. S9. Training effect of the $Mn_{3.5}Co_{0.5}N$ sample prepared with 87% excessive Co content. Consecutive hysteresis loops measured at 5 K (a)and 150 K (c) after field cooling under 1 T. H_{EB} as a function of cycling index number, N, at 5 K (b) and 150 K (d). Solid lines show the best fits with the powder-law to the data for N>1

III. MAGNETIC STRUCTURE DETERMINATION

We have performed symmetry analysis in order to determine the magnetic structures of $Mn_{3.5}Co_{0.5}N$. Starting with the parent space-group $Pm-3m1'$ and propagation vector **k** at the point of the Brillouin zone, through ISODISTORT, two active magnetic irreducible representations, mGM4+ and mGM5+, as well as their corresponding subgroups were obtained. The obtained magnetic structure models from the symmetry analysis were tested against neutron data by Rietveld refinement. We found that at 130 K, the canted AFM magnetic structure with magnetic symmetry R-3m′ transformed by irrep mGM4+ is the best solution, as presented in the main text and Fig. 1 (e). The so-called mGM5+ magnetic configuration with magnetic symmetry R-3m, usually employed to explain the NTE or magnetovolume effect in antiperovskites, is not suitable, as this solution does not allow the presence of magnetic Mn^{II}/Co at the corner site. Fig. S10 shows the refined result when considering mGM5+ transformed magnetic structure as well as a schematic drawing of the corresponding spin arrangement. Note that as we discussed in the main text, the NTE occurring at T_N=256 K is not associated with mGM5+ irrep, and instead mGM4+ is responsible for that. This indicates the $Mn_{3.5}Co_{0.5}N$ is distinct to the previous antiperovskites showing NTE effect, providing a unique case for the mechanism of NTE in this family.

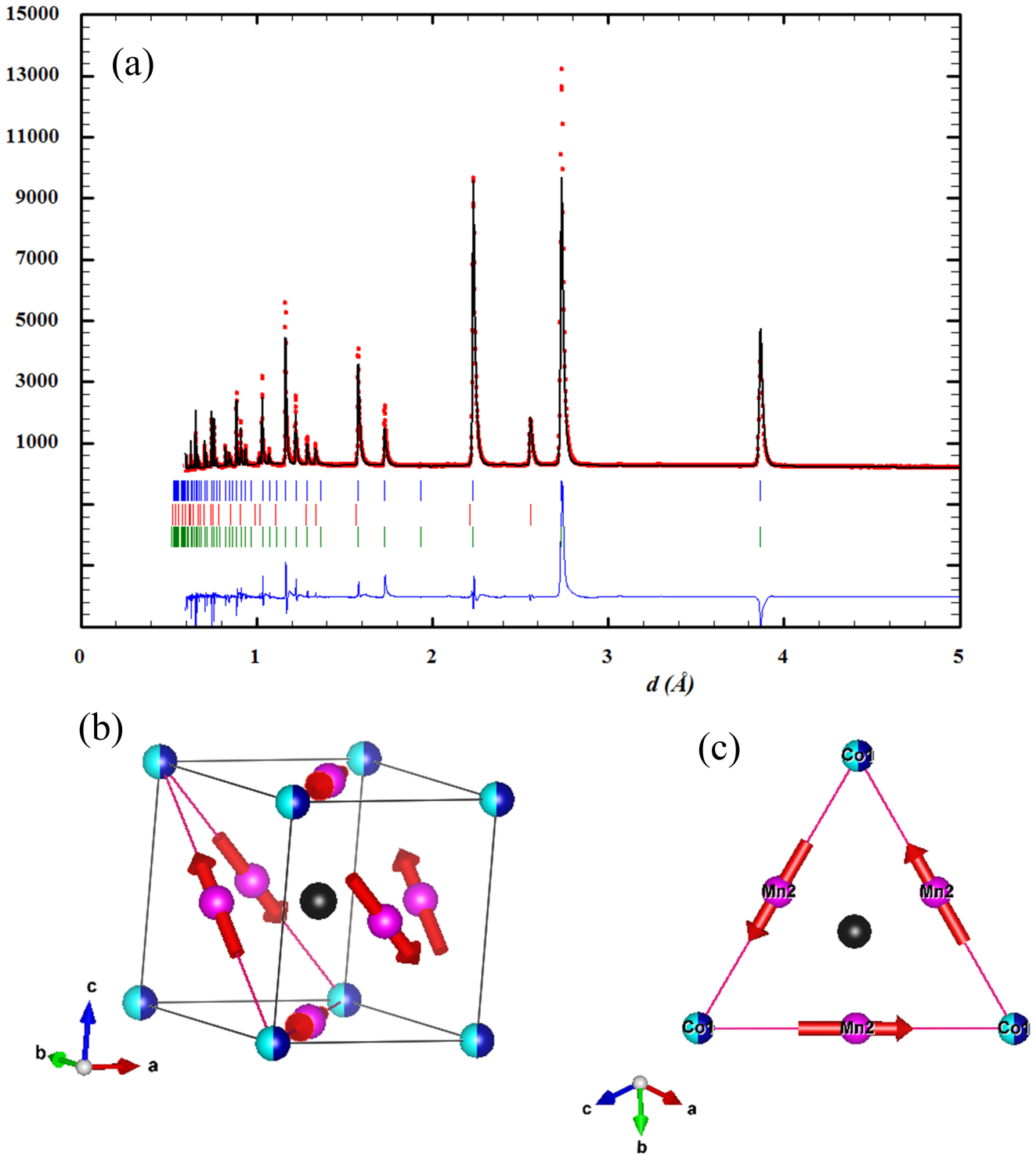

FIG. S10. (a) Observed (open circles) and calculated (line) powder neutron diffraction patterns collected at 130 K for the $Mn_{3.5}Co_{0.5}N$ sample prepared with 110% excessive Co content. The nuclear reflections are denoted by upper tick marks. The reflections marked in middle belong to a MnO impurity phase. The lowest tick marks show magnetic phase represented by mGM5+. The bottom line shows the difference between the observed and calculated patterns. (b) Schematic drawing for mGM5+ irrep magnetic structure.

IV. OTHER FIGURES

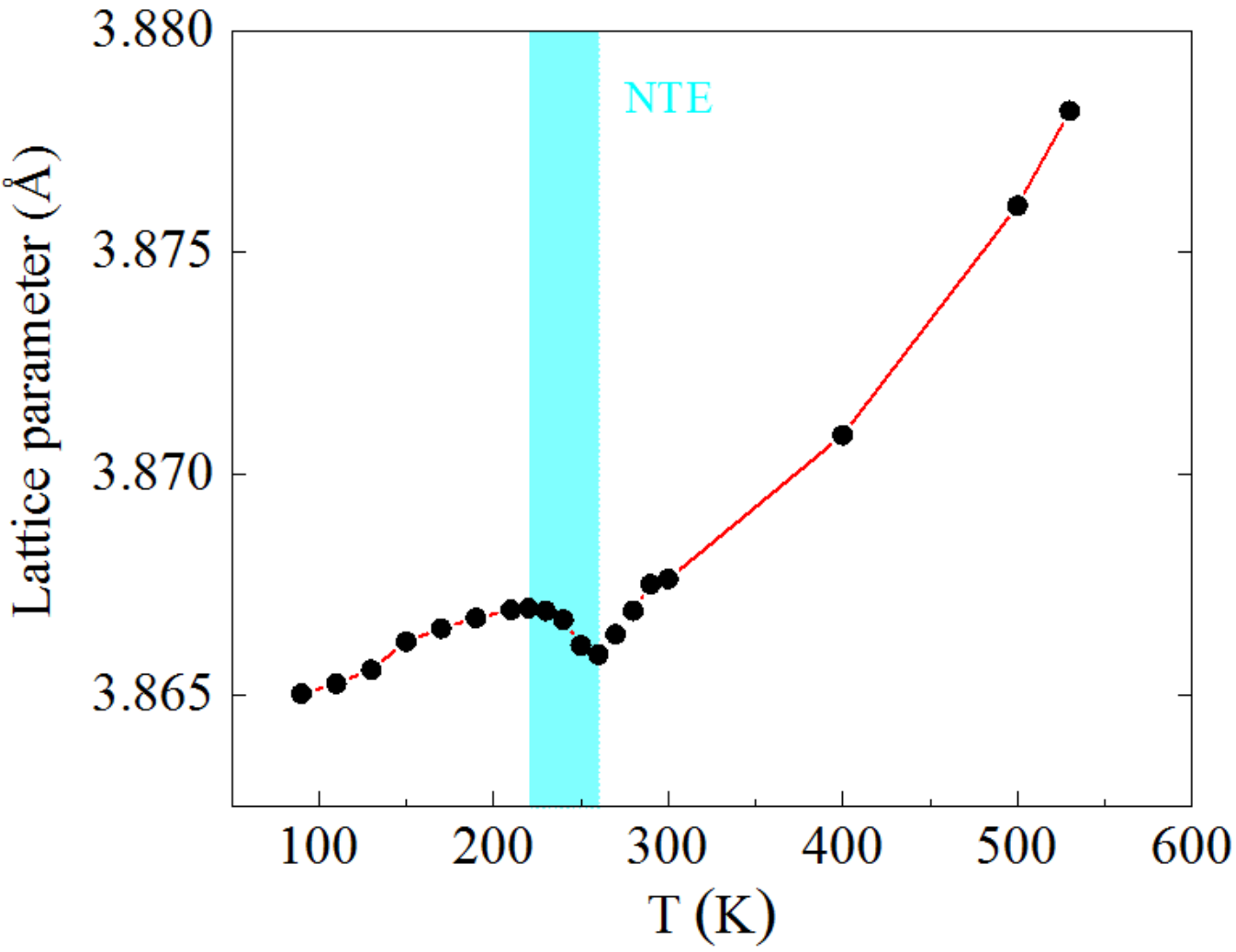

FIG. S11. Temperature dependence of the refined lattice parameter from NPD for the $Mn_{3.5}Co_{0.5}N$ sample prepared with 110% excessive Co content. The NTE zone is highlighted.

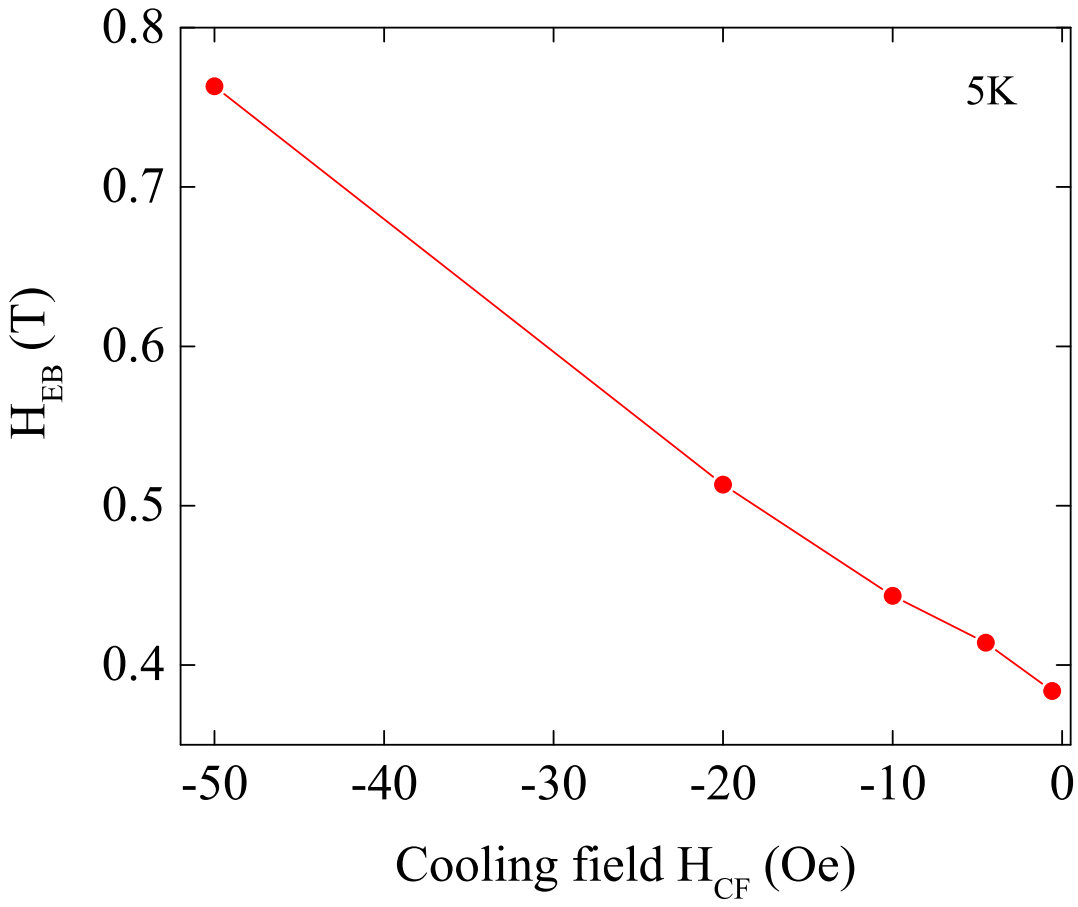

FIG. S12. Low-Cooling-field dependence of the H_{EB} of the $Mn_{3.5}Co_{0.5}N$ sample prepared with 110% excessive Co content at 5 K.

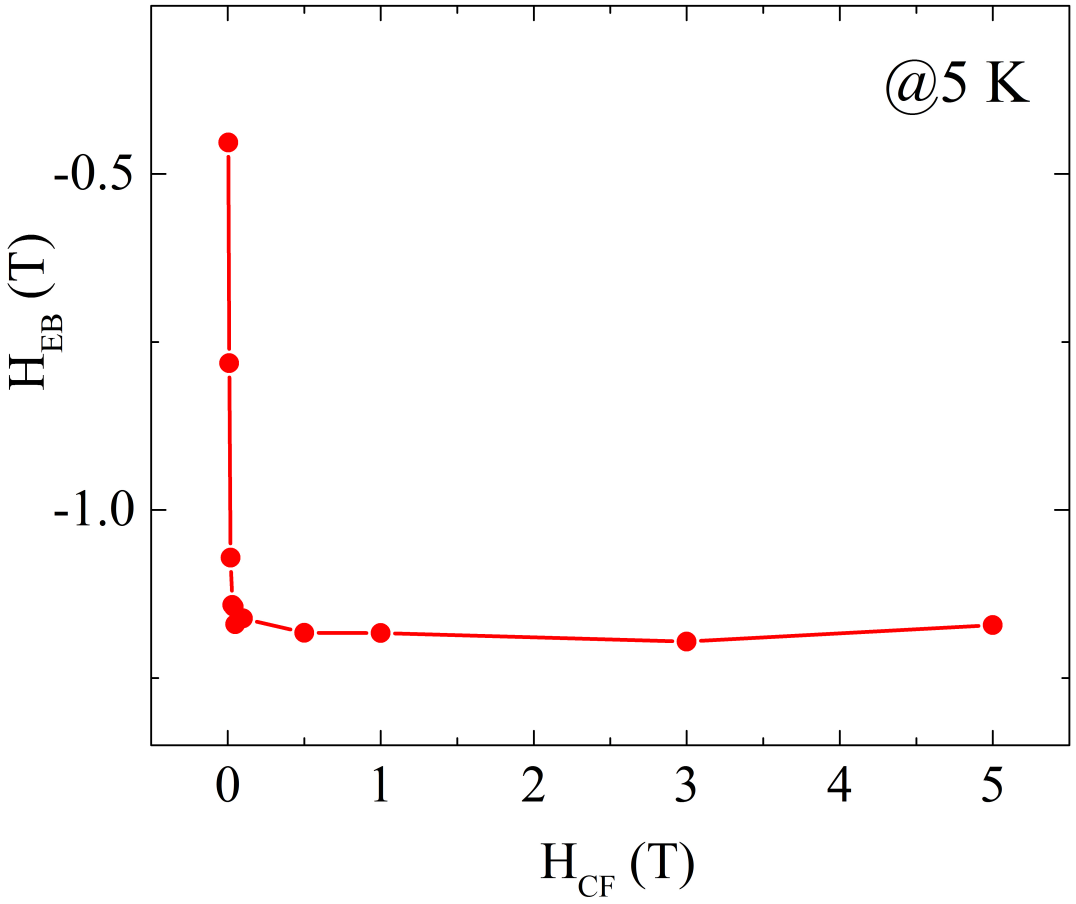

FIG. S13. Cooling-field-dependent of the H_{EB} of $Mn_{3.5}Co_{0.5}N$ sample prepared with 110% excessive Co content at 5 K.

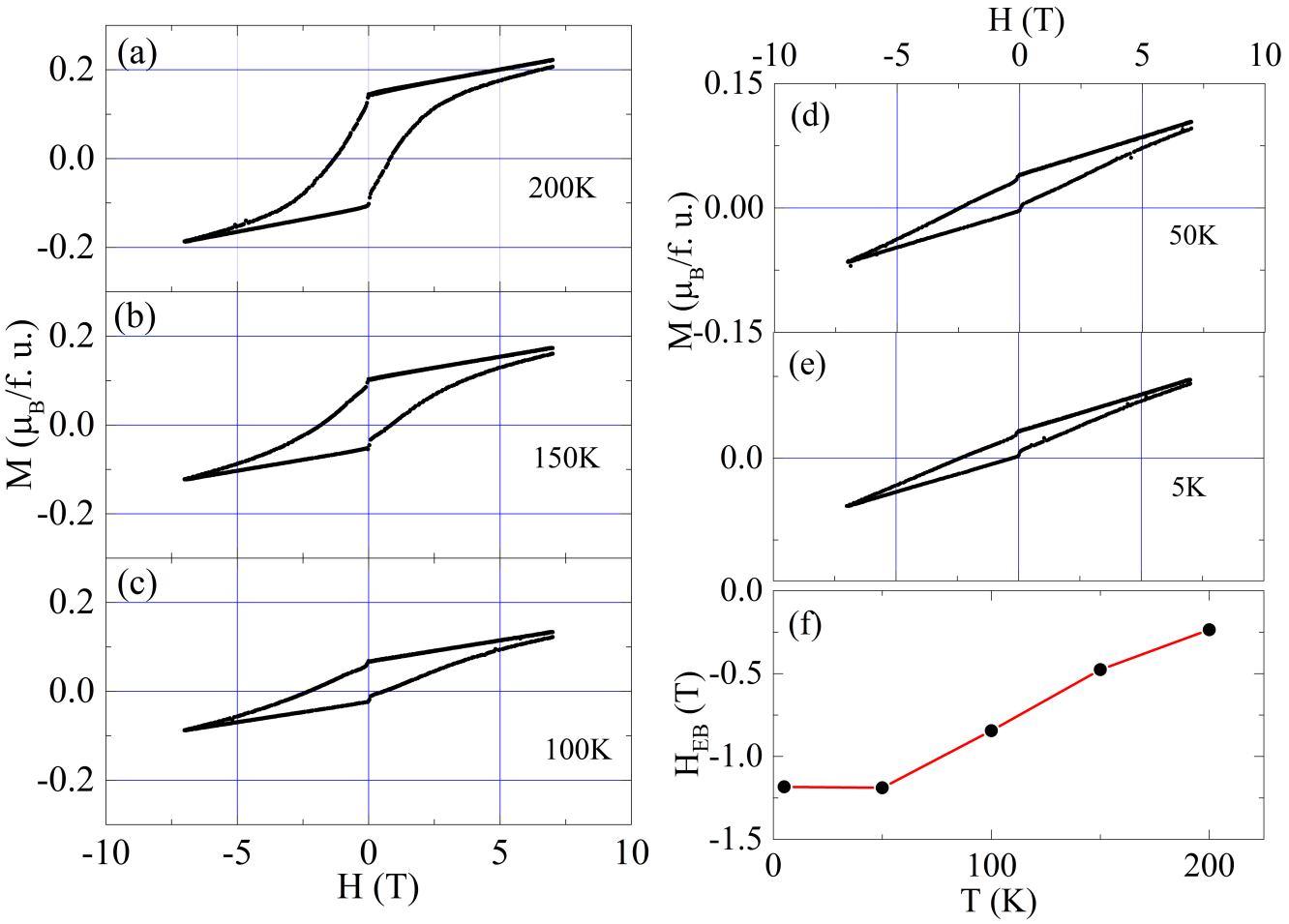

FIG. S14. (a)-(e) Magnetic hysteresis loops at different temperatures under a cooling field of 1 T as well as the temperature dependence of the value of H_{EB} under 1 T (f) for the $Mn_{3.5}Co_{0.5}N$ sample prepared with 110% excessive Co content.

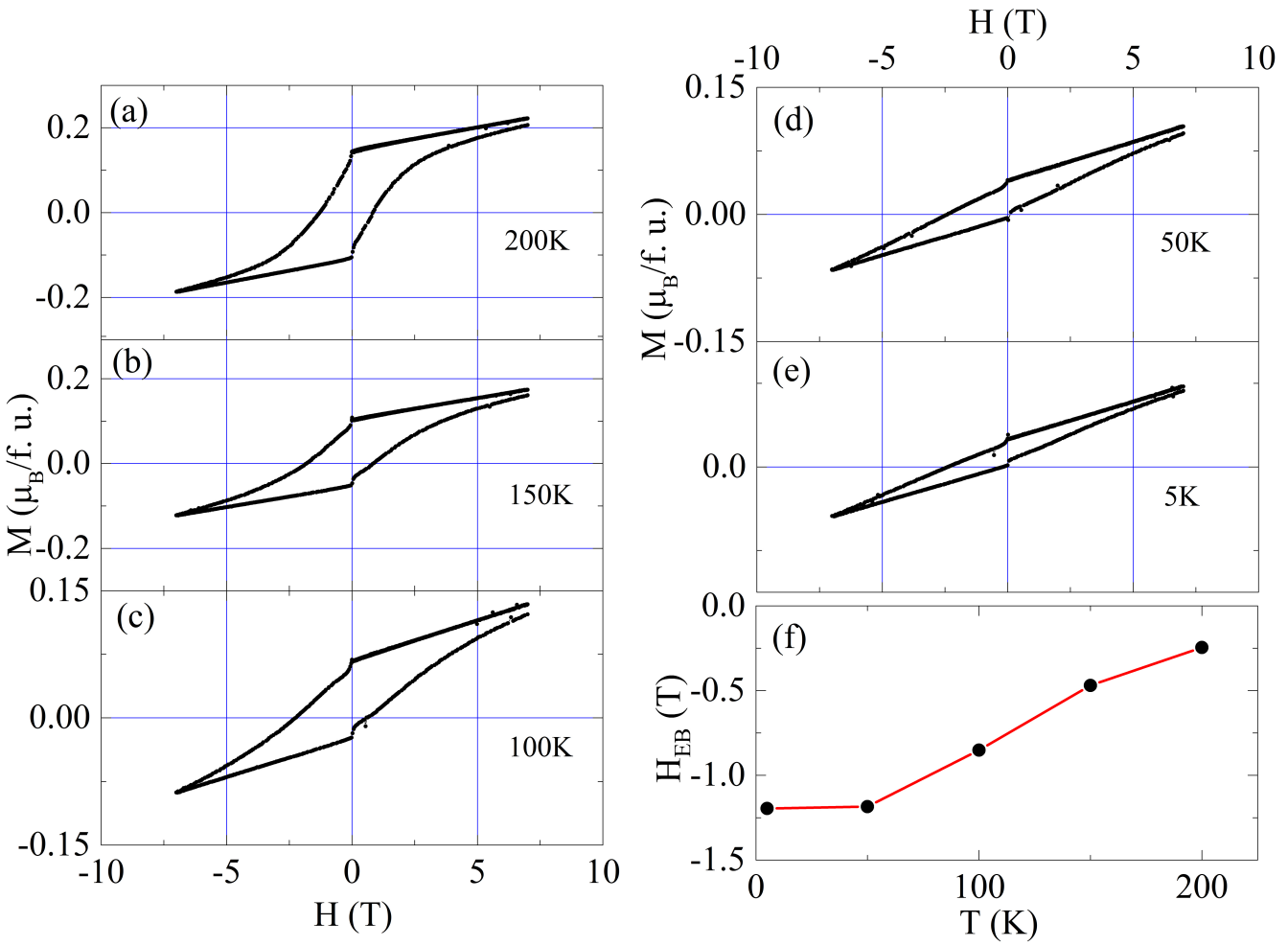

FIG. S15. (a)-(e) Magnetic hysteresis loops at different temperatures under a cooling field of 1 T as well as the temperature dependence of the value of H_{EB} under 3 T (f) for the $Mn_{3.5}Co_{0.5}N$ sample prepared with 110% excessive Co content.

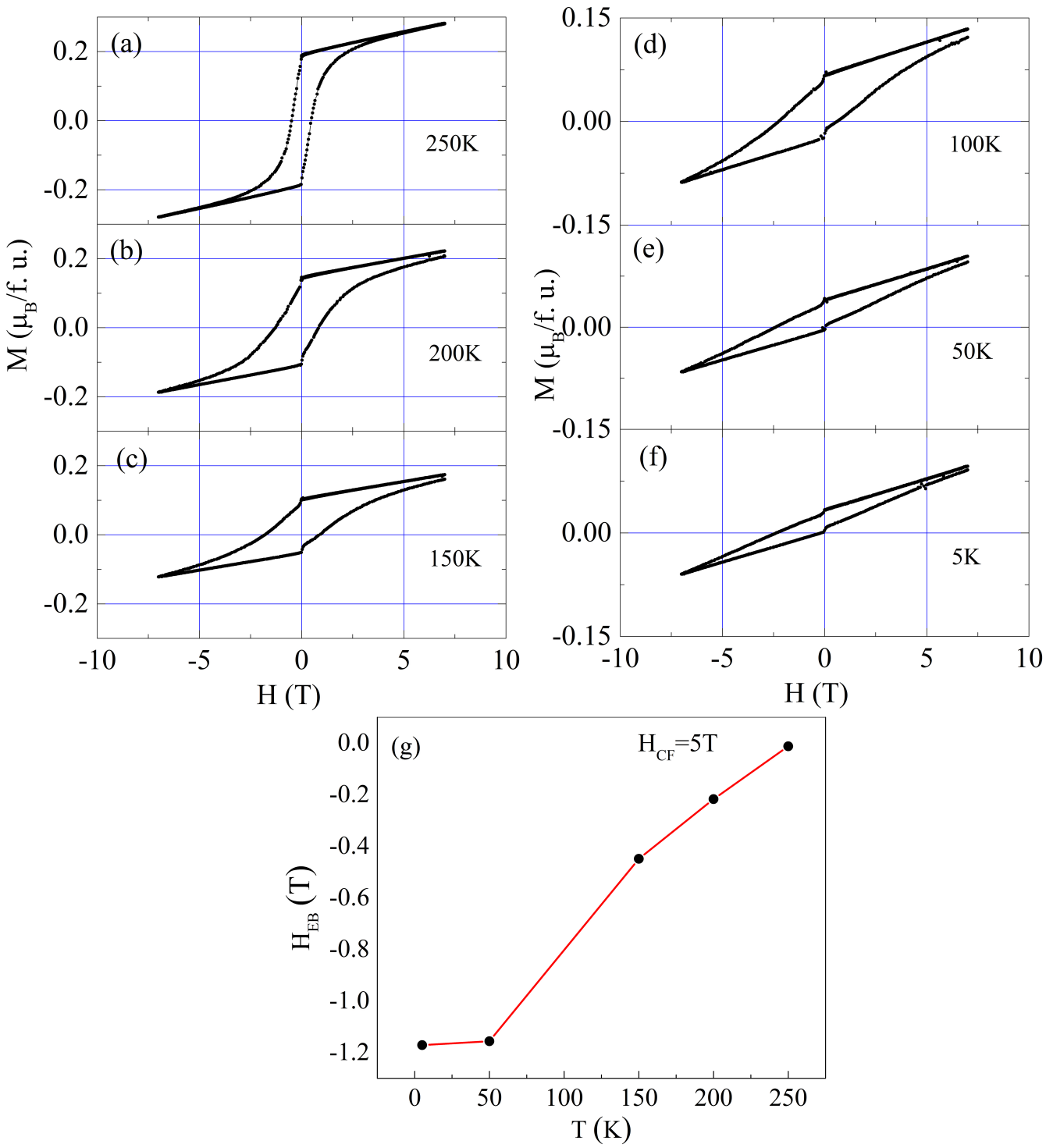

FIG. S16. (a)-(e) Magnetic hysteresis loops at different temperatures under a cooling field of 1 T as well as the temperature dependence of the value of H_{EB} under 5 T (f) for the $Mn_{3.5}Co_{0.5}N$ sample prepared with 110% excessive Co content.

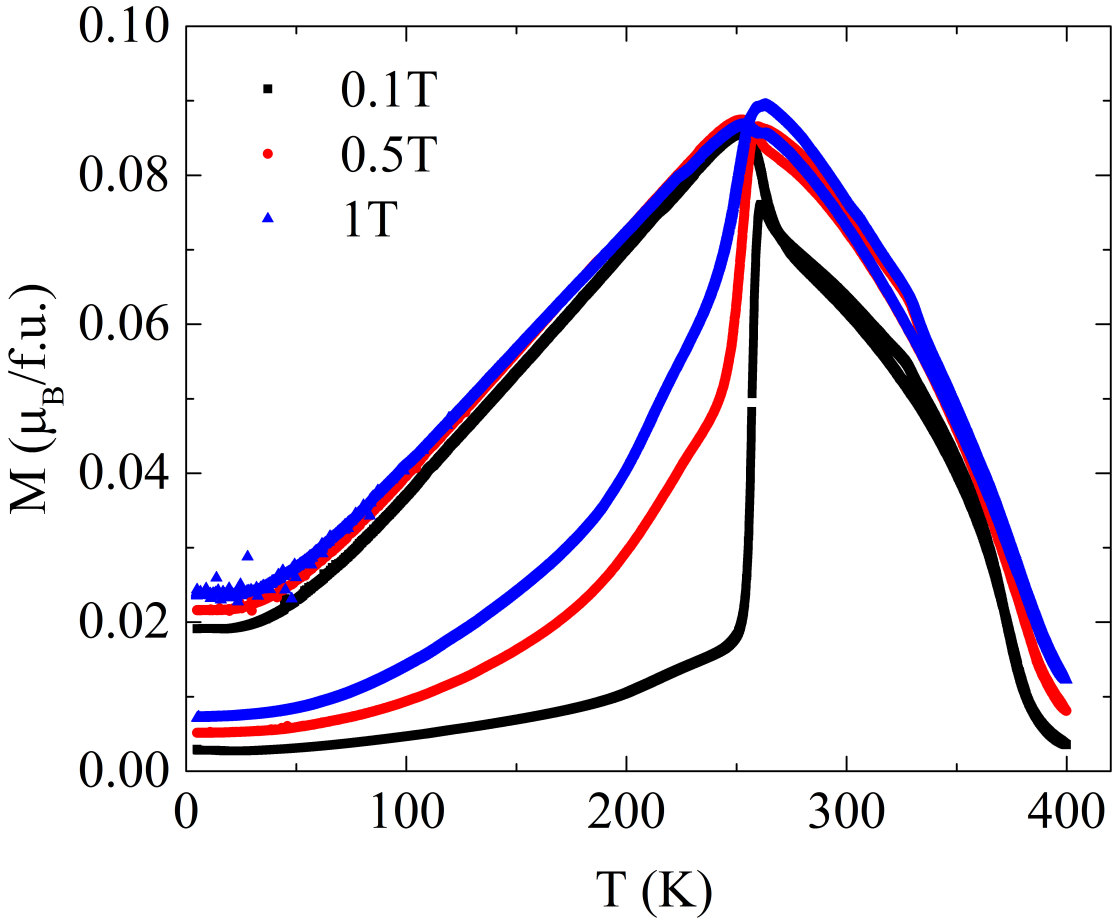

FIG. S17. Temperature dependence of the magnetization of the $Mn_{3.5}Co_{0.5}N$ sample prepared with 110% excessive Co content measured with ZFC and FC conditions under 0.1, 0.5 and 1 T